Disorder, screening, and quantum Hall oscillations

Keivan Esfarjani and Henry R. Glyde*
Department of Physics and Astronomy, University of Delaware, Newark, Delaware 19716

Virulh Sa-yakanit
Department of Physics, Faculty of Science, Chulalongkorn University, Bangkok 10500, Thailand
(Received 31 July 1989)

The density of states (DOS) of electrons in two-dimensional (2D) quantum wells and the broadening of Landau levels (LL's) is evaluated. The electrons are assumed to interact with screened, charged impurities located at random in the material. The random location of the impurities leads to a disordered environment seen by the electrons. The screening of the impurities by the 2D electron gas is evaluated in a simple Thomas-Fermi model which depends on the DOS at the Fermi surface, $n(E_F)$. The DOS and screening are evaluated iteratively at each magnetic field value. We find that the self-consistent evaluation of the DOS and screening leads to broadening of the LL's and $n(E_F)$ that oscillates with B. The oscillating LL widths and $n(E_F)$ are compared with the data of Heitmann *et al.*, Englert *et al.*, Wang *et al.*, and Smith *et al.* and reproduce all the observed values quite well. The chief adjustable parameter is the impurity concentration.

I. INTRODUCTION

Electrons confined to two dimensions (2D) display intriguing physical properties and have important device applications.[1-3] Typically, the electrons are confined to a plane (the x-y plane) at the interface between two materials (e.g., GaAs/$Al_xGa_{1-x}As$) or in multiple quantum wells (MQW's) formed by one material sandwiched between two others (e.g., InAs between GaSb). A magnetic field **B** is applied perpendicular to the x-y plane along the z axis. The material at or near the interface is doped (see Fig. 1). The impurities donate electrons which go to the interface to form a 2D electron gas (2D EG). The electrons interact with the remaining charged impurities which create a disordered environment.

Initial interest was chiefly in electron conductivity and localization. In the now-famous integer quantum Hall effect (IQHE), von Klitzing *et al.*[4] showed that the conductivity in the plane, σ_{xy}, rather than being a simple linear function of B, had plateaus of constant value, $\sigma_{xy}=(e^2/\hbar)i$, where i is an integer ($i=\ldots,3,2,1$). The plateaus in σ_{xy} occur when the Fermi energy E_F passes between the Landau levels (LL's) and through localized states, which do not contribute to the conductivity. The IQHE depends entirely on the existence of a substantial density of localized states between the LL's.

Recently, there has been much interest in properties such as cyclotron resonance[5-9] and thermodynamic properties[10-17] which depend on the total density of states (DOS) of the 2D EG. This includes both localized and extended states. These measurements show that the disorder, due to impurities[18] or to spatial inhomogeneities,[19] broadens the LL's significantly. They confirm that there is a large DOS between the LL's. Recent measurements[6-8,16,17] also display clearly that the broadening of the LL's oscillates with B. Essentially, the electrons in the 2D EG screen the charge of the impurities and therefore reduce the disorder. The effectiveness of the screening depends upon the DOS at the Fermi surface, $n(E_F)$. The magnitude of the disorder and the

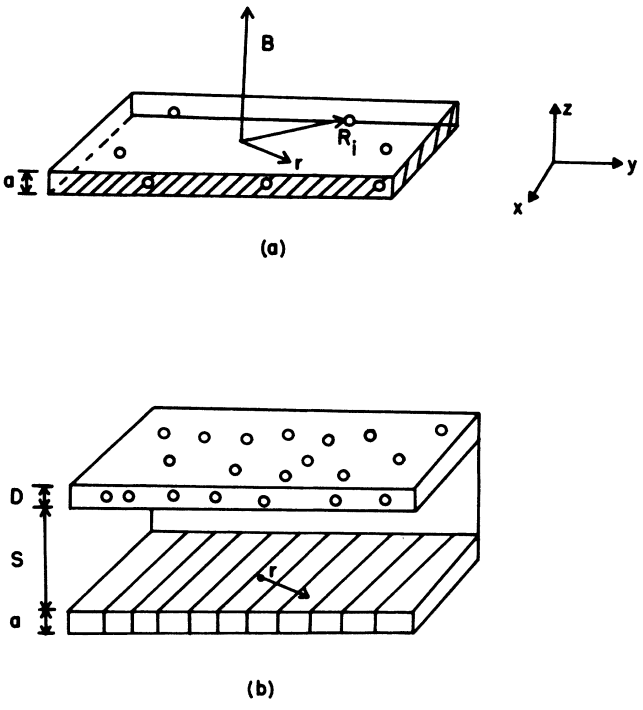

FIG. 1. (a) Schematic diagram of a 2D EG confined in a 2D quantum well, e.g., InAs sandwiched between GaSb. The dots represent impurities. (b) 2D EG confined to the interface between GaAs and $Al_xGa_{1-x}As$. The impurities are separated from the 2D EG by a spacer of pure material of thickness S.

broadening of the LL's caused by the impurities oscillates with oscillations in $n(E_F)$ as E_F sweeps through the LL's when B is increased.[20–25] We call this quantum Hall oscillations.

In a previous paper[26] we showed that a substantial DOS between LL's can be obtained using nonperturbative methods for electrons interacting with disorder having a finite correlation length L. In the model considered, the disorder was represented by the variance $W(r-r')=\langle V(r)V(r')\rangle$ of the disorder potential $V(r)$ seen by the electrons. The variance was modeled by a Gaussian,

$$W(r-r')=\xi_L e^{-(r-r')^2/L^2}, \tag{1}$$

in which the correlation length L and magnitude ξ_L are parameters. We found[26] that the observed[15] broadening could be reproduced with $L\approx 100$ Å and $\xi_L\approx 80$ meV^2. The origin of the disorder was not specified in the model, but LL broadening is generally believed to be due chiefly to charged impurities.[3,25] A model[19] which includes disorder due to sample inhomogeneities also predicts a substantial DOS between LL's.

The purpose of the present paper is to combine the previous[26] DOS expression with a model of impurity screening to obtain a self-consistent model of LL broadening due to screened impurities. We use a simple Thomas-Fermi (TF) model of the screening and identify the TF screening length with the correlation length L of the disorder. We consider both a three-dimensional (3D) and a 2D model of the screening. We find that for a two-dimensional electron system (2D ES) having a "width" $a=100$ Å or greater, the 2D model reduces to the 3D model and both give similar results. The DOS, $n(E)$, depends upon L and ξ_L. The variance (1) (L and ξ_L) depends upon $n(E_F)$. The $n(E)$, L, and ξ_L are evaluated iteratively until consistent. We compare the consistent values of $n(E_F)$ and the LL width directly with observed values from four experiments.[6,8,11,17] Some results for the 3D model have been presented previously.[27]

In Sec. II we discuss the DOS of the 2D EG interacting with disorder. In Sec. III we sketch the conventional 3D Thomas-Fermi model and develop a 2D TF model which is a simple extension, to quantum wells having a finite width, of the 2D model discussed by Ando *et al.*[3] Comparison is made with experiment in Sec. IV and the model and results are discussed in Sec. V.

II. DISORDER AND DENSITY OF STATES

An electron confined in the x-y plane in a MQW is an interesting example of a particle in a disordered environment.[28] The DOS of the electrons may be evaluated using several techniques developed for disordered systems. In the Born approximation,[3,18,20,25] a perturbative method, the DOS is elliptical around each LL and is zero between LL's. More exact methods[29–33] yield a Gaussian DOS for the lowest LL, as do path-integral methods.[34] We use a path-integral technique[26] developed[35,36] previously for electrons in disordered, bulk materials. Broderix *et al.*[37] discuss all these methods and the approximations in them carefully.

As in the IQHE, the electron-electron interaction may be ignored when evaluating the DOS, although it is included implicitly when screening is incorporated. We consider a single electron interacting with a disordered potential $V(r)=\sum_i v(r-R_i)$ where $v(r)$ is a screened electron-impurity ion potential. The impurity ions are randomly located (at R_i) creating fluctuations in $V(r)$. The Hamiltonian for this single electron in the x-y plane and a perpendicular magnetic field $\mathbf{B}=\nabla\times\mathbf{A}$ is[3]

$$H=H_0+V(r)=\frac{1}{2m}(\mathbf{p}+e\,\mathbf{A})^2+V(r)\ . \tag{2}$$

When $B=0$ and $V(r)=0$, the DOS per unit area for both spin states is a constant, $n(E)=n_0=m/\pi\hbar^2$. In a magnetic field B and $V(r)=0$, the electrons are confined to LL's having energy $E_n=\hbar\omega_c(n+\frac{1}{2})$ where $\omega_c=eB/m$ is the cyclotron frequency (we use rationalized SI units). The DOS is

$$n(E)=n_{\rm LL}\sum_n \delta(E-E_n)\ , \tag{3}$$

where $n_{\rm LL}=n_0\hbar\omega_c=1/\pi l^2=eB/\pi\hbar$ is the density of electrons that can be accommodated in a single LL. Here l is the cyclotron orbit radius, typically $l\sim 100$ Å. The LL's are depicted in Fig. 2. In the presence of impurities, the potential $V(r)$ seen by the electrons fluctuates from place to place due to fluctuations in the impurity concentration. Thus the total electron energy $[E=T+V(r)]$ fluctuates and not all electrons have the same energy. This broadens the LL's.

We assume the impurities are equally likely to be anywhere in the doped region [e.g., in a 3D model $\rho(R_i)=N/V=n_I$], where n_I is the impurity concentration and a is the MQW width [see Fig. 1(a)]. We set the average of $V(r)$ to zero [$\langle V(r)\rangle=0$] so that the electron energies remain centered at the LL energies. The variance or second moment,

$$W(r-r')=\langle V(r)V(r')\rangle = n_I\int d^3R_i\, v(r-R_i)v(r'-R_i)\ , \tag{4}$$

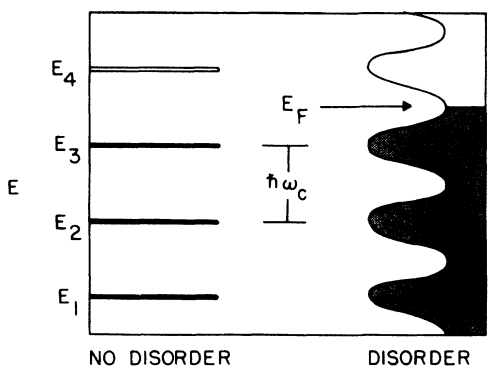

FIG. 2. The Landau levels for no disorder and broadened by disorder according to Eq. (6). The magnetic field B and electron density n_s in the figure is selected so that three LL's are completely filled (filling factor equals 6).

sets the magnitude of the fluctuations in $V(r)$. We model this by the Gaussian (1). We assume all higher moments of $V(r)$ are zero (all skewness is equal to 0), which leads to a DOS which is symmetric about the LL energies.

The derivation of the DOS for the above model using path-integral methods has been presented previously.[26,27] The resulting LL width Γ is

$$\Gamma^2=\xi_L\frac{x}{4+x}\ , \tag{5}$$

where $x=\hbar\omega_c/E_L=2eBL^2/\hbar$ and $E_L=\hbar^2/2mL^2$ is the kinetic energy of an electron localized within the correlation length L. The resulting DOS is a sum of Gaussians centered at each LL energy,[26]

$$n(E)=n_{\rm LL}(2\pi\Gamma^2)^{-1/2}\sum_n \exp\left[\frac{-(E-E_n)^2}{2\Gamma^2}\right]\ . \tag{6}$$

The DOS in (6) is depicted in Fig. 2. Previously, we found (6) agreed well with the DOS observed by Eisenstein *et al.*[15] in GaAs/$Ga_xAl_{1-x}As$ heterostructures if $L\approx 100$ Å and $\xi_L=80$ (meV)^2. Using $m=0.06m_e$, the LL separation is $\hbar\omega_c=6$ meV at $B=3$ T. The DOS (5) and (6) is the same as obtained by Gerhardts[34] for $n=0$.

In the ground state, the lowest LL's are occupied up to the Fermi energy E_F given by

$$n_s=\int_0^{E_F} dE\, n(E)\ , \tag{7}$$

where $n_s=N/A$ is the electron density. From (6), the electron density that can be occupied in a single LL remains at $n_{\rm LL}=n_0\hbar\omega_c=eB/\pi\hbar$. We define a filling factor ν_F as[3]

$$\nu_F=2i\equiv 2\frac{n_s}{n_{\rm LL}}=\frac{n_s h}{eB}=n_s 2\pi l^2\ . \tag{8}$$

When $\nu_F=2$ we can accommodate all the electrons in the lowest LL. When $\nu_F=2,4,6,\ldots$ the LL's are completely filled and E_F lies between two LL's [where $n(E)$ is small]. The case $\nu_F=6$ is depicted in Fig. 2. When $\nu_F=1,3,5,\ldots$, the highest occupied LL is half-filled and E_F lies at the center of that LL where $n(E)$ is a maximum. The $n_{\rm LL}$ in $n(E)$ depends upon B. Thus, from (7), E_F will decrease as B is increased and we expect $n(E_F)$ to oscillate as E_F sweeps down through the LL's. Since the screening length is proportional to $n(E_F)$, we expect the screening length to oscillate with B. When we identify the correlation length L with the screening length, we expect Γ in (5) to oscillate with B. This leads to the observed oscillation of Γ discussed in Sec. IV.

The white-noise (WN) limit of $W(r-r')$, in which $L=0$, is interesting,

$$W_{\rm WN}\equiv\lim_{L\to 0}\left[\frac{W(L)}{\pi L^2}e^{-(r-r')^2/L^2}\right]$$
$$=W(0)\delta(r-r')\ . \tag{9}$$

The WN variance has zero range and may be obtained from (4) for a potential which has zero range (a contact potential). Comparing (1) and (9) we have

$$\lim_{L\to 0}\xi_L=\frac{W(0)}{\pi L^2} \tag{10}$$

which suggests that $\xi_L\sim L^{-2}$ as $L\to 0$. In the WN limit, the LL width in (5) reduces to the contact-potential result,[3]

$$\Gamma^2_{\rm WN}=\xi_L x/4=\tfrac{1}{2}n_0\hbar\omega_c W(0)\ .$$

III. DISORDER AND SCREENING

In the preceding section, we set out the DOS, $n(E)$, of electrons in a disordered environment caused by randomly located, charged impurities. The disorder was described entirely by the variance $W(r-r')$ in the impurity potential. This variance was modeled by the Gaussian function (1) have screening length L and magnitude ξ_L as free parameters. Our goal here is to evaluate $W(r-r')$ for random impurities screened by the 2D EG and so establish ξ_L and L. We use a simple TF model of the screening.

We wish to compare with experiments which have different geometries and locations of the impurities. For example, the 2D EG in practice has a width, typically[8,17] of $a=80$–200 Å. When the width is larger than the screening length (q_s^{-1}) we find a simple 3D TF model is appropriate. That is, if we begin with a 2D model, as discussed, for example, by Ando *et al.*,[3] then for $a>q_s^{-1}$ the variance calculated using the 2D model reduces to the 3D result. In the samples used by Wang *et al.*[17] and Smith *et al.*,[11] the impurities are separated from the 2D EG by a spacer of pure material of height $S\approx 200$–500 Å. When $S\gg q_s^{-1}$, we find that the correlation length L depends on S (i.e., on how far the impurities are from the 2D EG) and becomes independent of q_s^{-1}. In this case a 2D model taking account of the nature of the heterojunction is more realistic. We now evaluate $W(r-r')$ for the 3D and 2D cases.

A. Three-dimensional model

We picture wide quantum wells in which the impurities are distributed at random, both within the quantum well and in the material on each side. A 3D model assumes that the electrons respond equally in all directions. The variance $W(r-r')$ for three dimensions has been evaluated by Halperin and Lax.[37] We sketch the argument to contrast the 2D models.

We begin with Poisson's equation,

$$-\nabla^2\phi(r)=\frac{1}{\epsilon}\rho(r)=\frac{1}{\epsilon}[\rho_{\rm ext}(r)+\rho_{\rm ind}(r)]\ , \tag{11}$$

for the electric potential $\phi(r)$ seen by an electron at r due to an external charge density $\rho_{\rm ext}(r)$. In (11) $\rho_{\rm ind}(r)$ is the charge density induced in the EG by $\phi(r)$. We consider a single (external) charged impurity at the origin, $\rho_{\rm ext}(r)=Ze\delta(r)$. In the TF approximation,[3]

$$\rho_{\rm ind}(r)=-e[N_V(E-\mu-e\phi(r))-N_V(E-\mu)]$$
$$\approx -e\frac{dN_V}{d\mu}e\phi(r)=-e^2n_V(E_F)\phi(r)\ ,$$

where N_V is the 3D electron number density and $n_V(E_F)$ is the 3D DOS at E_F. Introducing the Fourier transform

$$\phi(r)=\int \frac{d^3q}{(2\pi)^3} e^{iq\cdot r}\phi(q) ,$$

Poisson's equation becomes

$$\phi(q)=\frac{Ze}{\epsilon}\frac{1}{q^2+Q_s^2} , \tag{12}$$

where

$$Q_s^2\equiv\frac{e^2}{\epsilon}n_V(E_F)=\frac{e^2}{a\epsilon}n(E_F) \tag{13}$$

is the Thomas-Fermi wave vector (inverse of the TF screening length). In the last part of (13) we have used $n_V(E_F)=a^{-1}n(E_F)$ to relate the 3D to the 2D DOS (see Fig. 1). The potential $v(r)=-e\phi(r)$ due to the impurity is

$$v(r)=-\int \frac{d^3q}{(2\pi)^3} e^{iq\cdot r}\frac{Ze^2}{\epsilon}\frac{1}{q^2+Q_s^2}=-\frac{Ze^2}{4\pi\epsilon}\frac{e^{-Q_s r}}{r} . \tag{14}$$

This $v(r)$ may be thought of as an electron-impurity ion potential. The variance due to N such impurities distributed uniformly throughout volume V with density $\rho(R_i)=n_I=N/V$ is

$$\begin{aligned} W(r-r')&\equiv n_I\int d^3R_i\, v(r-R_i)v(r'-R_i) \\ &=\int \frac{d^3q}{(2\pi)^3} e^{iq\cdot(r-r')} n_I|v(q)|^2 \\ &=2\pi\left[\frac{Ze^2}{4\pi\epsilon}\right]^2 n_I Q_s^{-1} e^{-Q_s|r-r'|} . \end{aligned} \tag{15}$$

From (15) the Fourier component of the variance is

$$W(q)=n_I v(q)^2=n_I\left[\frac{Ze^2}{\epsilon}\right]^2\frac{1}{(q^2+Q_s^2)^2} . \tag{16}$$

Comparing (15) with the Gaussian variance (1) it is natural to identify Q_s^{-1} with the correlation length L and ξ_L with the magnitude in (15). That is,

$$L=Q_s^{-1}=\left[\frac{e^2}{\epsilon a}n(E_F)\right]^{-1/2} \tag{17}$$

and

$$\xi_L=2\pi\left[\frac{Ze^2}{4\pi\epsilon}\right]^2 n_I L . \tag{18}$$

Equations (17) and (18) combined with the DOS results (5), (6), and (7) for $n(E_F)$ constitute the 3D model. Clearly L and ξ_L are proportional to $n(E_F)^{-1/2}$. We therefore expect L and $\Gamma^2=\xi_L x/(4+x)$ to oscillate with B as E_F sweeps through the LL's. We find $Q_s^{-1}\approx 100$ Å^{-1}, which is less than $a=200$ Å for the samples used by Heitmann *et al.*[8] The 3D model is implemented in Sec. IV.

B. Two-dimensional screening

Screening for 2D heterostructures in the TF approximation has been discussed by Ando *et al.*[3] We generalize their treatment to consider a 2D EG having a small but finite width a. We seek a 2D electron-impurity ion interaction $v(r)$, where $r=x,y$ is now a 2D variable lying in the plane of the 2D EG, from which we may calculate a 2D variance $W(r-r')$. We begin again with Poisson's equation (11) for the electric potential $\phi(z)$ seen by the electrons and write the 3D number density in it as

$$N_V(r,z)=n_s(r)f(z) .$$

Here z lies perpendicular to the plane, $n_s(r)$ is the number density per unit area in the plane, and $f(z)$ is the density along z perpendicular to the plane. We take $f(z)$ as fixed and unresponsive to any external charge. Possible models are $f(z)=\delta(z)$, $f(z)=\frac{1}{2}b^3z^2e^{-bz}$, and $f(z)=(\pi/2a)\sin(s\pi/a)$. We simply take $f(z)$ as uniform along z [$f(z)=1/a$, $-a\le z\le 0$], or

$$f(z)=\frac{1}{a}[\theta(z+a)-\theta(z)] . \tag{19}$$

We found we could not get good agreement with experiment taking $a=0$ [$f(z)=\delta(z)$].

In Poisson's equation, (11),

$$-\nabla^2\phi(r,z)=\frac{1}{\epsilon}[\rho_{\rm ext}(r,z)+\rho_{\rm ind}(r,z)] ,$$

the induced charge is now

$$\begin{aligned} \rho_{\rm ind}(r,z)&=-e[n_s(E-\mu-e\phi(r,z))-n_s(E-\mu)]f(z) \\ &\approx -e^2n(E_F)\phi(r,z)f(z) . \end{aligned} \tag{20}$$

To obtain a 2D variance, we seek a 2D electric potential $\bar{\phi}(r)$ independent of z. We choose to define this as

$$\bar{\phi}(r)\equiv\int dz\,\phi(r,z)f(z) . \tag{21}$$

For a constant $f(z)$, as in (19), $\bar{\phi}(r)$ is simply an average of $\phi(r,z)$ over the width of the 2D EG. We replace $\phi(r,z)$ in (20) by $\bar{\phi}(r)$, i.e.,

$$\rho_{\rm ind}(r,z)=-e^2n(E_F)\bar{\phi}(r)f(z) . \tag{22}$$

Equation (22) makes it clear that the 2D EG charge density cannot respond along the z axis but is fixed at $f(z)$. Poisson's equation is then

$$-\nabla^2\phi(r,z)+2q_sf(z)\bar{\phi}(r)=\frac{1}{\epsilon}\rho_{\rm ext}(r,z) ,$$

where

$$q_s\equiv\frac{e^2}{2\epsilon}n(E_F)=\frac{a}{2}Q_s^2 \tag{23}$$

is the 2D screening length discussed, for example, by Ando *et al.*[3] To solve (23) we introduce the Fourier transforms,

$$\phi(r,z)=\int\frac{d^2q}{(2\pi)^2}\int\frac{dk}{2\pi}e^{i(q\cdot r+kz)}\phi(q,k)\ ,$$
$$\bar{\phi}(r)=\int\frac{d^2q}{(2\pi)^2}e^{iq\cdot r}\bar{\phi}(q)\ , \tag{24}$$
$$f(z)=\int\frac{dk}{2\pi}e^{ikz}f(k)\ .$$

The definition of $\bar{\phi}(r)$ in (21) becomes

$$\bar{\phi}(q)=\int\frac{dk}{2\pi}f(-k)\phi(q,k)\ . \tag{25}$$

Substituting (24) into Poisson's equation, we obtain

$$(q^2+k^2)\phi(q,k)+2q_sf(k)\bar{\phi}(q)=\frac{1}{\epsilon}\rho_{\rm ext}(q,k)\ . \tag{26}$$

The chief difference between (26) and the 3D result (12) is the mixed appearance of $\phi(q,k)$ and $\bar{\phi}(q)$ in (26).

To obtain an equation for $\bar{\phi}(q)$ only, we divide (26) by (q^2+k^2), multiply it by $f(-k)$, and integrate over k. Using (25) this gives

$$\bar{\phi}(q)+\frac{q_s}{q}F(q)\bar{\phi}(q)=\bar{\phi}_{\rm ext}(q)\ , \tag{27}$$

where

$$F(q)\equiv 2q\int\frac{dk}{2\pi}\frac{f(-k)f(k)}{q^2+k^2}$$
$$=\int dz\int dz'\,f(z)f(z)e^{-k|z-z'|}\ ,$$
$$\bar{\phi}_{\rm ext}(q)\equiv\frac{1}{\epsilon}\int\frac{dk}{2\pi}\frac{f(-k)\rho_{\rm ext}(q,k)}{q^2+k^2}\ .$$

Introducing the dielectric function $\epsilon(q)=[1+(q_s/q)F(q)]$, Eq. (27) takes the familiar form

$$\bar{\phi}(q)=\frac{1}{\epsilon(q)}\bar{\phi}_{\rm ext}(q)\ . \tag{28}$$

The 2D electron-impurity ion potential is $v(q)=-e\bar{\phi}(q)$.

To proceed, we specialize to a constant charge density along z given by (19) for which

$$f(k)=\frac{i}{ka}(1-e^{ika})\ ,$$
$$F(q)=\frac{2}{(qa)^2}(e^{-qa}+qa-1)\ , \tag{29}$$

and to a single charge impurity a height Z_i above the 2D EG, $\rho_{\rm ext}(r,z)=Ze\delta(r)\delta(z-Z_i)$ [$\rho_{\rm ext}(q,k)=Ze\,e^{-ikZ_i}$] for which

$$\bar{\phi}_{\rm ext}(q)=\frac{Ze}{\epsilon}f(iq)\frac{e^{-qZ_i}}{2q}$$
$$=\frac{Ze}{2\epsilon a}(1-e^{-qa})\frac{e^{-qZ_i}}{q^2}\ . \tag{30}$$

Substituting these results into (28), the 2D electron-impurity potential [$v(q)=-e\bar{\phi}(q)$] is

$$v(q)=-\left[\frac{Ze^2}{2\epsilon a}\right]\frac{(1-e^{-qa})e^{-qZ_i}}{q^2\epsilon(q)}\equiv v'(q)e^{-qZ_i}\ . \tag{31}$$

Given $v(r)$ we may be evaluate a variance $W(r-r')$ due to impurities substituted at random positions (R_i,Z_i). From (4) this is

$$W(r-r')=n_I\int dZ_i\int d^2R_i\,v(r-R_i)v(r'-R_i)$$
$$=n_I\int dZ_i\int\frac{d^2q}{(2\pi)^2}e^{iq\cdot(r-r')}v'(q)^2e^{-2qZ_i}\ . \tag{32}$$

In the last line above we have carried out the average over the impurity positions R_i parallel to the plane. As noted the impurities may be separated a distance S from the 2D EG within a doped region of width D [see Fig. 1(b)]. In this case the integral in (32) is

$$\int dZ_i\,e^{-2qZ_i}\to\int_S^{S+D}dZ_i\,e^{-2qZ_i}=\frac{e^{-2qS}}{2q}(1-e^{-2qD})$$

and

$$W(r-r')=\int\frac{d^2q}{(2\pi)^2}e^{iq\cdot(r-r')}W(q) \tag{33}$$

with

$$W(q)=n_I\left[\frac{Ze^2}{2\epsilon a}\right]^2\frac{e^{-2qS}}{2q}\frac{(1-e^{-2qD})(1-e^{-qa})^2}{q^4[\epsilon(q)]^2}\ . \tag{34}$$

The variance (34) clearly depends on several lengths; the 2D screening length q_s^{-1}, the width of the 2D EG, S, and on D. Typically in GaAs/Al_xGa_{1-x}As quantum wells, we find q_s^{-1} oscillates about the value $q_s^{-1}\sim 45$ Å. To identify the correlation length we consider limits of $W(q)$. We find that the size of D turns out to be not very important in $W(q)$ in establishing L and we can choose $D=\infty$ or $D=0$. In the limits below, we take $D=\infty$, for example.

C. Limits of the 2D variance

We now explore limits of the variance (34).

1. *Wide 2D EG ($a\gg q_s^{-1}$) and no spacer [$S=0$ ($S\ll q_s^{-1}$)]*

In this case $F(q)\to 2/aq$, $(1-e^{-qa})\to 1$, $q^4\epsilon(q)^2\to(q^2+2q_s/a)^2=(q^2+Q_s^2)^2$, and (34) reduces to

$$W(q)=n_1b^2\frac{1}{2q}\frac{1}{(q^2+Q_s^2)^2}\ , \tag{35}$$

where $b^2=(Ze^2/2\epsilon a)$. For $a\gg q_s^{-1}$ we therefore recover essentially the 3D model in which Q_s^{-1} is the scaling or correlation length, $L\sim Q_s^{-1}\sim[n(\epsilon_F)]^{-1/2}$. The $W(q)$ in (35) differs slightly from (16) because (35) is two dimensional and we have not allowed the 2D EG to respond along the z direction.

2. *Narrow 2D EG ($a\ll q_s^{-1}$) and no spacer ($S=0$)*

In this limit $F(q)\to 1$, $q^4\epsilon(q)^2\to q^2(q+q_s)^2$, $(1-e^{-qa})^2\to(aq)^2$, and (34) becomes

$$W(q)=n_Ib^2a^2\frac{1}{2q}\frac{1}{(q+q_s)^2}\ . \tag{36}$$

Introducing the dimensionless variable $x=q/q_s$, the variance is

$$W(r)=\frac{n_I b^2 a^2}{q_s}\int \frac{d^2x}{(2\pi)^2} e^{iq_s x\cdot r}\frac{1}{2x(1+x)^2}\ , \tag{37}$$

and it is natural to identify the correlation length as

$$L\sim q_s^{-1}\sim[n_s(E_F)]^{-1}\ . \tag{38}$$

In this limit, L is the 2D screening length[3] q_s^{-1}.

3. Wide spacer ($S\gg q_s^{-1}$)

In this limit the value of a is not critical and we take $a\ll q_s^{-1}$. The $W(q)$ is the same as (36) except for e^{-2qS}, i.e.,

$$W(q)=n_I b^2 a^2\frac{e^{-2qS}}{2q}\frac{1}{(q+q_s)^2} \tag{39}$$

and

$$W(r)=\frac{n_I b^2 a^2}{4\pi q_s}\int_0^\infty dx\, J_0(q_s r x)\frac{e^{-2q_s Sx}}{(1+x)^2}\ ,$$

where $J_0(\alpha x)=(2\pi)^{-1}\int_{-\pi}^{\pi} d\theta\, e^{i\alpha\sin\theta}$ is the zeroth-order Bessel function. When S is large, only small x contributes to the integral $[(1+x)\approx 1]$ and

$$W(r)=\frac{n_I b^2 a^2}{8\pi S q_s^2}\frac{1}{[1+(r/2S)^2]^{1/2}}\ . \tag{40}$$

In this limit

$$L\sim S\ . \tag{41}$$

Thus for large $S\gg q_s^{-1}$, the correlation length becomes independent of q_s^{-1} and depends upon how far the impurities are separated from the 2D EG. For $S\gg q_s^{-1}$, but $a\gg q_s^{-1}$, we get the same result (40) except for a factor of 4.

Finally, to establish ξ_L we could use the above limits. However, we choose ξ_L so that the "volume" of the variance given by the Gaussian (1) is the same as the "volume" given by the full $W(r-r')$ in (34). That is,

$$\xi_L\int d^2r\, e^{-r^2/L^2}=\int d^2r\, W(r)=W(q=0)\ ,$$

which using (34) gives

$$\xi_L=\frac{1}{\pi L^2}W(q=0)=\frac{n_I D}{\pi L^2}\left[\frac{Ze^2}{2\epsilon}\right]^2\frac{1}{q_s^2}\ . \tag{42}$$

This has the advantage that ξ_L is independent of S and a and is the same for all the above limits. The important parameter in ξ_L is the product $n_I D$ and the important functional dependence is q_s^{-2}. Thus ξ_L can depend on the screening length q_s^{-1} even for large S when L does not.

D. Models for 2D screening

Given the 2D Thomas-Fermi expression (33) for $W(r-r')$ and the above limits, we proposed the following simple models for the correlation length L in (1).

1. No spacer ($S=0$)

For no spacer,

$$L=\left[q_s^{-2}+\frac{a}{2q_s}\right]^{1/2}\ . \tag{43}$$

For a narrow 2D EG ($a\to 0$), (43) becomes $L\to q_s^{-1}$ which is the screening length discussed by Ando *et al.*[3] for $a=0$. For a wide 2D EG ($a\gg q_s^{-1}$), (43) is $L\to(a/2q_s)^{1/2}=Q_s^{-1}$ which is the 3D TF screening length. For the quantum wells considered here $a\geq 100$ Å and we find $q_s^{-1}\sim 45$ Å.

2. Spacer ($S\neq 0$)

For a spacer,

$$L=\begin{cases}(S^2+Q_s^{-2})^{1/2}, & q_s^{-1}<a \qquad (44)\\ (S^2+q_s^{-2})^{1/2}, & q_s^{-1}>a\ . \qquad (45)\end{cases}$$

For short screening lengths $q_s^{-1}\ll S$, $L\to S$ and L becomes independent of q_s. In all cases, we have determined ξ_L, using (42), as

$$\xi_L=\frac{n_I D}{\pi L^2}\left[\frac{e^2}{2\epsilon q_s}\right]^2+\xi_0\ . \tag{46}$$

A constant value ξ_0 was added to reflect contributions to ξ_L from other disorder. The ξ_0 also helps to stabilize the iterative solution by preventing ξ_L from vanishing during the iterations. The ξ_L in (46) has the correct (white-noise) limit (10) for $L\to 0$.

IV. COMPARISON WITH EXPERIMENT

Properties of MQW's such as cyclotron resonance and magnetocapacitance depend on the total density of states. Specifically, the linewidth, Γ_c, of the cyclotron resonance observed by Englert *et al.*[6] and by Heitmann *et al.*[8] is proportional to the width Γ of the LL's. From heat capacity measurements, Wang *et al.*[17] and Smith *et al.*[11] have extracted Γ and the density of states at the Fermi surface, $n(E_F)$, respectively. In this section we evaluate Γ and $n(E_F)$ using the DOS and screening models of Secs. II and III for direct comparison with these four measurements. The input parameters characterizing the samples in each case, such as electron density n_s, 2D EG width a, and the impurity concentration n_I, that we have used are listed in Table I. The parameters with an asterisk are not fixed by experiment but were adjusted here to get the best agreement with experiment.

As noted in Sec. II, the width of the LL's is given by (5) and the DOS is given by (6), in which $n_{\rm LL}=n_0\hbar\omega_c=eB/\pi\hbar$ is the density of electrons that can be accommodated in a single LL. The electrons fill the lowest LL's up to the Fermi energy E_F given by (7). Clearly, E_F depends upon B since the density accommodated in a single LL, $n_{\rm LL}$, is proportional to B. In Sec.

TABLE I. Sample parameters used in the 2D Thomas-Fermi screening model. The parameters are dictated by the experiment except the values with an asterisk, which are free parameters. The important free parameter in the model is the product $n_I D$.

Reference	Fig.	$q_s^{-1}(B=0)$ (Å)	n_S (10^{11} cm^{-2})	$\frac{m}{m_e}$	$\frac{\epsilon}{\epsilon_0}$	a (Å)	S (Å)	D (Å)	n_I (10^{17} cm^{-3})	$\frac{\xi_0}{\xi_L(B=0)}$	$\frac{\xi_0}{(\text{meV})^2}$
Wang *et al.*	9	45	8.8	0.0664	11	175	200	40*	2*	0.4	3.0
Smith *et al.*	10	45	1.9	0.066	11	100*	500	55	1*	0.55	0.5
Englert *et al.*	11	45	1.2	0.069	11	100*	0	80*	0.12*	3	12.7
Heitmann *et al.*	12	90	8.8	0.0374	15	180	0	50*	1*	0.5	6.7

III we developed models for the variance parameters L and ξ_L in (1). The L and ξ_L clearly depend upon the DOS at E_F, $n(E_F)$. To implement this sequence, we solve Eqs. (5), (6), and (7) iteratively with models for L and ξ_L appropriate to the sample geometry used in the four experiments set out in Table I.

A. 3D model

In this model we combine Eqs. (5)–(7) for the DOS with the 3D Thomas-Fermi model, leading to Eqs. (17) and (18) for L and ξ_L, respectively. To set the stage, we show in Fig. 3 the DOS obtained by iterating these equations at fixed $B=6$ T for the sample characteristics of Heitmann *et al.*,[8] a wide 2D EG. The $n(E)$ is clearly a sum of Gaussians peaked at the centers of the LL's. The adjustable parameter is the impurity concentration n_I. This was adjusted to obtain the amplitude of Γ which agreed best with the experiment[8] ($n_I=1.1\times10^{17}$ cm^{-3}).

In Fig. 4 we show the correlation length obtained as a function of B. At small B, the separation between the LL's, $\hbar\omega_c=\hbar eB/m$, is small and $n(E)$ is approximately a constant, $n_0=m/\pi\hbar^2$. Thus $n(E)$ is independent of E and $n(E_F)$, given by (6), is independent of B. This makes L independent of B even though E_F is decreasing with increasing B. As B gets larger, the LL's separate and $n(E_F)$ and L begin to oscillate with B as E_F moves down through the LL's. The correlation length (screening length) is a maximum when E_F lies between two LL's (at even filling factors), where $n(E_F)$ is a minimum. The amplitude of the oscillations in L increases with B.

The corresponding calculated width Γ given by (5) is compared with Γ_c observed by Heitmann *et al.*[8] in Fig. 5. From (5) we expect Γ to be proportional to $\sqrt{B}$ at low B ($\Gamma^2\approx\xi_L x/4$ when $x\ll4$). At large B ($x\gg4$) we expect the mean value of Γ to become independent of B. This general behavior is displayed in Fig. 5. Clearly, the amplitude and phase of the oscillations agree well with those in Γ_c which is proportional to Γ. The maximum values of Γ occur at even filling factors when the LL's are completely filled. From Fig. 4, the 3D screening length is typically $Q_s^{-1}=L\sim50$–100 Å. This is less than the

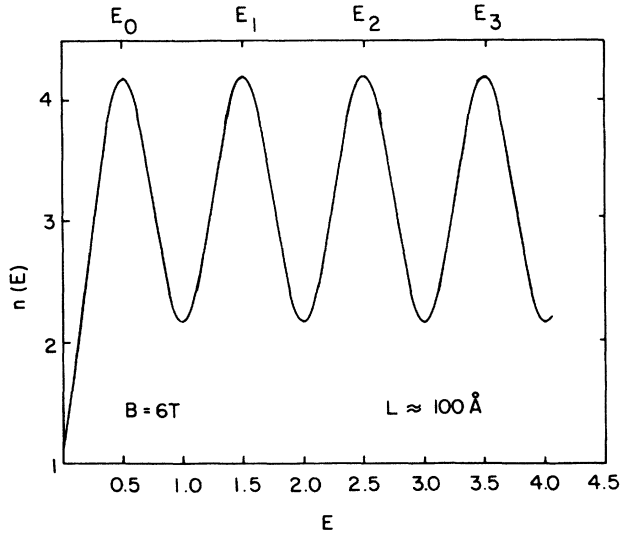

FIG. 3. DOS obtained from (6) and the 3D Thomas-Fermi model at $B=6$ T using $\epsilon=15\epsilon_0$, $a=200$ Å, and $n_I=1.1\times10^{17}$ cm^{-3} giving $L\approx100$ Å and $\xi_L\approx80$ (meV)^2.

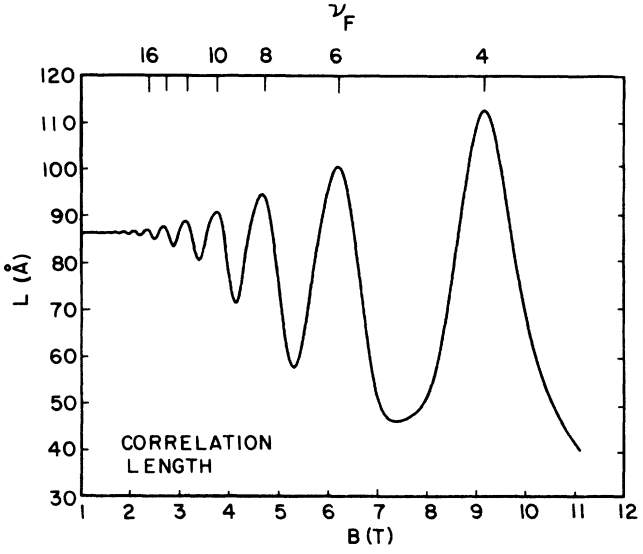

FIG. 4. The correlation length L vs magnetic field obtained from the 3D Thomas-Fermi model, with sample geometry used by Heitmann *et al.* ($a=180$ Å, $n_I=1.1\times10^{17}$ cm^{-3}).

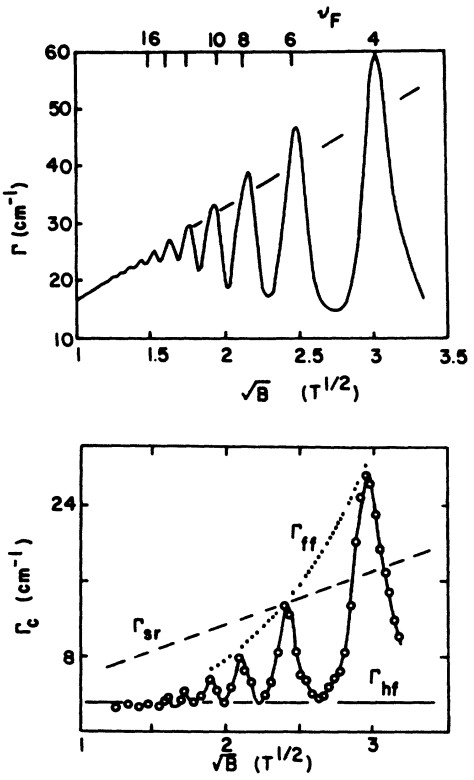

FIG. 5. Upper half: LL width Γ vs $\sqrt{B}$ calculated using the 3D Thomas-Fermi model. As $B \to 0$, $\Gamma \propto \sqrt{B}$. Lower half: Cyclotron resonance width observed by Heitmann *et al.* (Ref. 8).

width of the 2D EG, $a = 200$ Å, used by Heitmann *et al.* Also, the impurities are probably distributed at random through the 2D EG making a bulk, 3D model reasonable.

In Fig. 6 we compare the 3D model Γ with the Γ extracted by Wang *et al.*[17] from their measurements of the specific heat. Our calculated Γ in Fig. 6 is the same as that shown in Fig. 5 but plotted on a different scale. Clearly the calculated and observed Γ's agree well. Since the impurities are separated from the 2D EG by a spacer in the samples used by Wang *et al.*, a simple bulk 3D model may not be appropriate.

B. 2D models

Here we combine Eqs. (4)–(6) for the DOS with the 2D Thomas-Fermi values for L and ξ_L derived in Sec. III B. We begin with an arbitrary value of the LL width Γ and evaluate the following equations:

$$n(E) = \frac{n_{\mathrm{LL}}}{(2\pi\Gamma^2)^{1/2}} \sum_{n=0}^{\infty} \exp\left[-\frac{(E-E_n)^2}{2\Gamma^2} \right], \tag{6'}$$

$$n_s = \int_0^{E_F} n(E)\,dE \quad (\text{for } E_F), \tag{7'}$$

$$q_s = \frac{e^2}{2\epsilon} n(E_F), \quad Q_s^2 = \frac{e^2}{a\epsilon} n(E_F), \tag{23'}(13')$$

$$L = L(S, q_S, Q_s) \tag{44'}$$

$$= \begin{cases} (S^2 + Q_s^{-2})^{-1/2} & (\text{Figs. 9 and 10}) \\ (q_S^{-2} + Q_s^{-2})^{1/2} & (\text{Figs. 11 and 12}), \end{cases} \tag{43'}$$

$$\xi_L = \frac{n_I D}{\pi L^2 q_s^2} \left[\frac{Ze^2}{2\epsilon} \right]^2 + \xi_0, \tag{46'}$$

$$\Gamma^2 = \xi_L \frac{x}{4+x}, \quad x = \frac{2eBL^2}{\hbar}. \tag{5'}$$

Equations (5')–(7'), (13'), (23'), (43'), (44'), and (46') were evaluated iteratively until consistent. For samples having a spacer (samples of Wang *et al.*[17] and Smith *et al.*[11]), we used Eq. (44') for L [Eq. (44)]. When there was no spacer (samples of Englert *et al.*[6] and Heitmann *et al.*[8]) we used Eq. (43') for L [Eq. (43)]. The resulting consistent values of q_s^{-1} for the samples used by Wang *et al.*, are shown in Fig. 7. There we see that q_s^{-1} oscillates

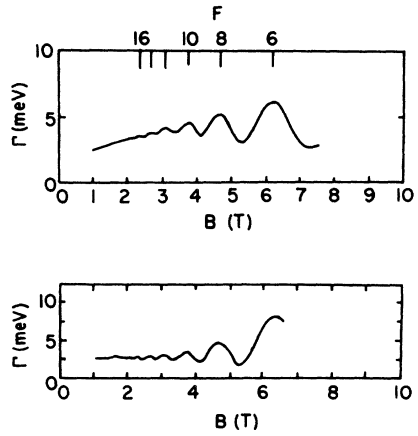

FIG. 6. Upper box: Width of the LL's, Γ, calculated using the Gaussian DOS (6) and the 3D screening model, Eqs. (17) and (18). Lower box: Γ extracted from C_V data by Wang *et al.* (Ref. 17).

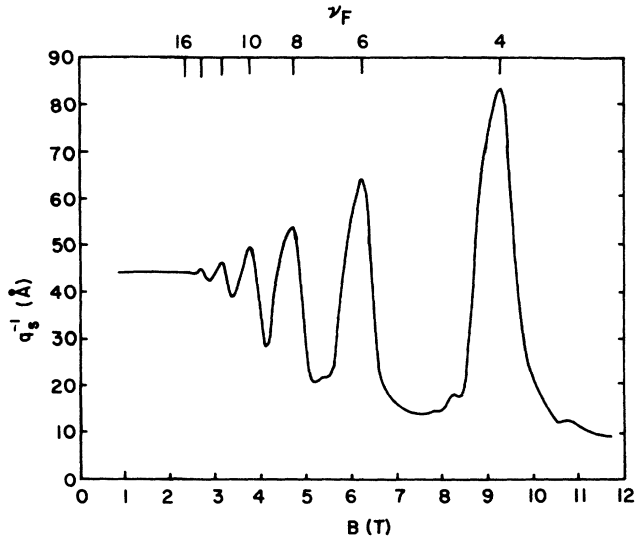

FIG. 7. The 2D Thomas-Fermi screening length q_s^{-1} obtained from self-consistent solution of the 2D Thomas-Fermi model for samples used by Wang *et al.* (Ref. 17).

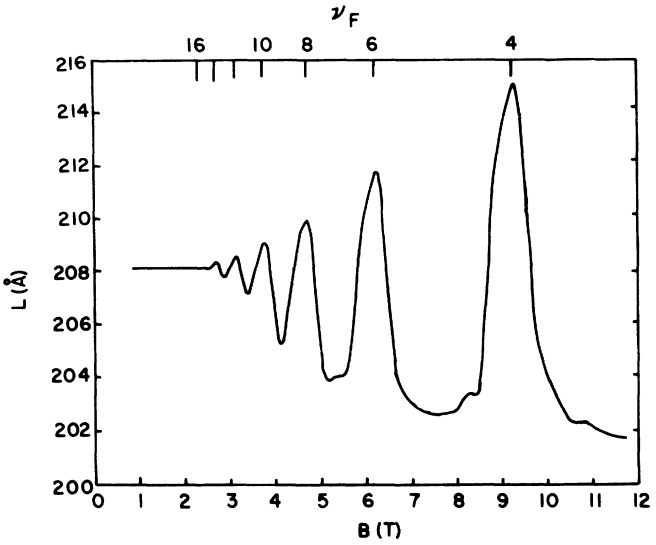

FIG. 8. As Fig. 7 for the correlation length, L, using $S=200$ Å.

with the magnetic field and is generally less than 100 Å. The corresponding values of the correlation length L, given by (44), are shown in Fig. 8. Clearly, when there is a spacer, L is dictated chiefly by the spacer thickness, S.

In Fig. 9 we compare Γ for the 2D model with that extracted from the heat capacity by Wang *et al.*[17] The sample characteristics we have used in the calculation are set out in Table I. From Fig. 9 we see that the calculated Γ agrees well in magnitude and in amplitude of the oscillations with the observed Γ. The calculated Γ appears to have a minimum value of $\Gamma\approx 2.2$ meV. The impurity density we have used is $n_I=2\times 10^{17}$ cm^{-3} in the doped region. When multiplied by $D=40$ Å, the product $n_I D$ we have used is 15 times smaller than the value quoted by Wang *et al.*

The DOS at E_F observed by Smith *et al.* and our evaluated $n(E_F)$ for their sample geometry are compared in Fig. 10. For $B\to 0$ we expect $n(E_F)\to n_0=m/\pi\hbar^2$. As B increases the LL's separate, E_F sweeps down through the LL's, and $n(E_F)$ oscillates with B. The amplitude of the oscillations in $n(E_F)$ will increase with B as the LL's separate. These general features are seen in Fig. 10 and the calculated $n(E_F)$ reproduces the observed value well. The important free parameter is again the product Dn_I and this was adjusted to get the correct amplitude of $n(E_F)/n_0$.

In Fig. 11, we compare the cyclotron linewidth observed by Englert *et al.*[6] with our calculated LL width Γ. For samples used by Englert *et al.*,[6] D and n_I were not specified so that the product Dn_I is again an adjustable parameter. We assumed $a=100$ Å. With these values of Dn_I and a, the 2D TF model with the DOS (6) repro-

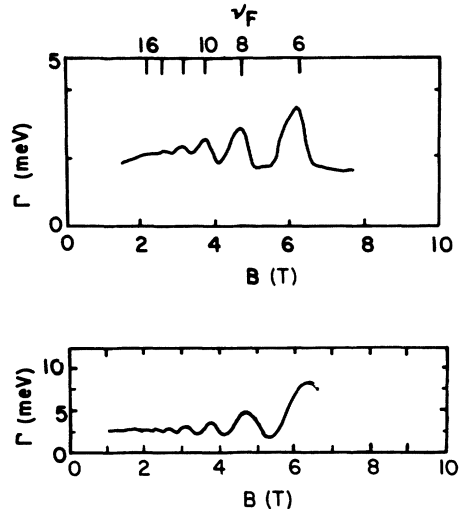

FIG. 9. Width of the LL's, Γ, calculated using the Gaussian DOS and the 2D screening model, Eqs. (5')–(7'), (13'), (23'), (43'), (44'), and (46'), compared with the Γ obtained from heat capacity data by Wang *et al.* (Ref. 17).

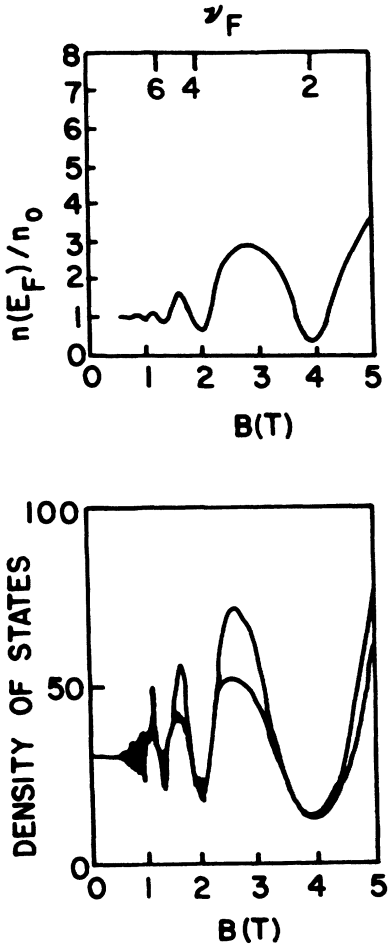

FIG. 10. The DOS at E_F, $n(E_F)$, compared with that observed by Smith *et al.* (Ref. 11).

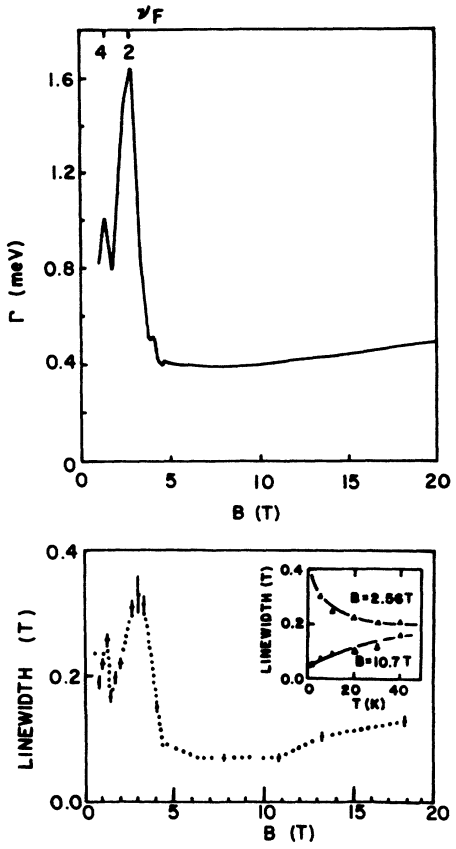

FIG. 11. The width of the LL's, Γ, compared with the cyclotron resonance linewidth Γ_C observed by Englert *et al.* (Ref. 6).

duces the oscillations in the observed linewidth Γ_c.

Finally, in Fig. 12 we compare the 2D model Γ obtained using (43) for L with that observed by Heitmann *et al.* Again the product Dn_I is an adjustable parameter. Clearly, Figs. 5 and 12 are very similar showing that the 3D and 2D models give similar results for samples in which $a \gg q_s^{-1}$. Typically, we find $q_s^{-1} \sim 45$ Å so that indeed $a \gg q_s^{-1}$ in these samples. Then the chief difference between the 2D and 3D models is that the 2D EG cannot respond along the z direction in the 2D model. The similarity of Figs. 5 and 12 suggests that this restriction does not affect the final results greatly.

V. DISCUSSION

From the comparison with four separate experiments in Figs. (9)–(12), we see that the present model of the DOS and TF screening describes 2D quantum wells quite accurately. This appears to confirm the basic interpretation[20–25] that the oscillations in the LL widths are due to oscillations in the screening of the disorder by the electrons in the 2D EG. The present model is quite simple but has some essential features. Firstly, the DOS is evaluated nonperturbatively. Thus the DOS $n(E)$ for large values of $(E - E_n)$ can be obtained. The DOS can therefore be finite for all E and does not vanish between LL's. Secondly, $n(E)$ is evaluated for arbitrary correlation length L of the disorder. This corresponds to electron-impurity ion potentials $v(r - R_i)$ having a finite range. This allows us to relate L to the screening length. This would not be possible had we considered a contact electron-impurity ion potential which leads to the white-noise variance ($L = 0$) given by (9). The present evaluation of the DOS using path integrals is a generalization of the self-consistent Born approximation (SCBA), for contact potentials in two ways. Firstly, a nonperturbative $n(E)$ which is finite at all E is obtained. Secondly, $n(E)$ for potentials having a finite and variable range (finite L) is obtained. The importance of using a finite-range potential has recently been stressed by Ando and Murayama.[23] The Thomas-Fermi model is clearly an oversimplification, particularly in a magnetic field. However, it has a length, the screening length, which we can identify with L. The magnitude ξ_L can also be related to the variance calculated in the TF model. We find $L \approx 100$ Å which is not small on atomic dimensions.

The comparison with the cyclotron resonance width observed by Heitmann *et al.* in QW's having a width $a \approx 200$ Å is especially interesting. In this case we find a is approximately twice the screening length and the 2D and 3D TF models give the same value for L, the 3D TF screening length $L = Q_s^{-1}$. Only ξ_L, given by (18) and (46), differs. For this QW, the good agreement with ex-

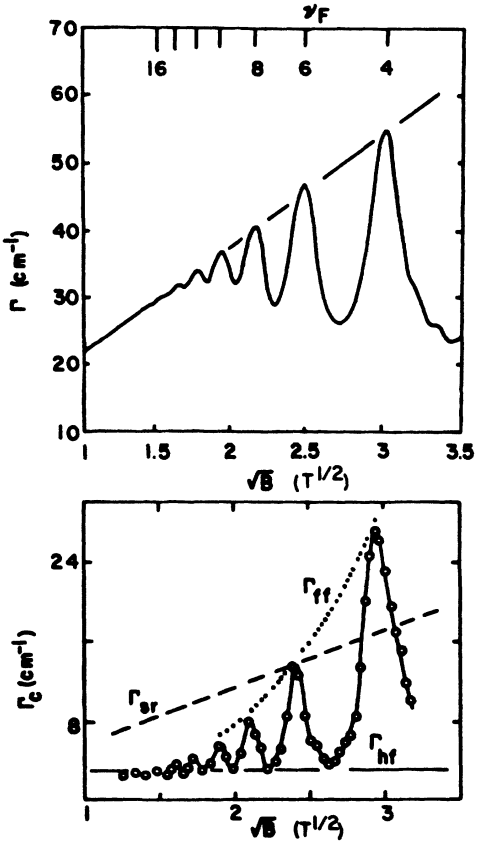

FIG. 12. The LL width, Γ, calculated using the 2D Thomas-Fermi model compared with the cyclotron resonance linewidth Γ_C observed by Heitmann *et al.* (Ref. 8).

periment in Figs. 5 and 12 is independent of the details of the screening model. A large value of ξ_0 was required in the 2D model.

The chief free parameter in the screening model is the impurity concentration n_I (or the product $n_I D$ in the 2D model) appearing in ξ_L. The results were sensitive to n_I. If a very large value of n_I is selected, ξ_L and Γ will be large and $n(E)$ will go to a constant and oscillations in $n(E_F)$ and L will be damped. If a small value is selected, Γ will decrease and $n(E)$ will vanish between LL's leading to large amplitude oscillations in L and $n(E_F)$. There is therefore an optimum value of n_I leading to realistic oscillations. Generally, quite large values of n_I were needed to obtain good agreement with experiment. However, in the one case in which $n_I D$ was given by experiment,[17] our optimum model value was less than the observed value. The 2D model appears to be most appropriate for samples having a spacer of pure material separating the impurities from the 2D EG. For $a > Q_s^{-1}$ and no spacer, the 3D model is most appropriate. In all cases we found it important to retain a finite value of the QW width.

To obtain the Gaussian DOS (6) we made approximations. Particularly, we took[26,27] the long-time limit of the electron propagator which means $n(E)$ is valid for the lowest-lying Landau levels only. This approximation probably masks difficulties that appear with the DOS for higher LL's. These questions are carefully discussed by Broderix *et al.*[37]

Finally, we have worked here via a Gaussian model of the variance. This is restrictive and perhaps not necessary. It would be interesting to evaluate the DOS using the TF model variance (34) directly, perhaps numerically. The variance (34) contains much more information than the Gaussian variance (1). Including higher moments of $V(r)$ could also change the shape of $n(E)$. For example, numerical calculations[38] of the DOS suggest that $n(E)$ need not be symmetric around the LL's. The TF model of $\epsilon(q)$ is valid only in the long-wavelength limit ($q \ll 2k_F$). This limit is fulfilled if $L^{-1} < 2k_F \sim \sqrt{\nu_F / l_c}$, which is valid for the present materials, especially those with large spacers. Experiments in which the 2D EG width a or the spacer width were varied systematically would also be interesting to test the model.

ACKNOWLEDGMENTS

It is a pleasure to acknowledge valuable discussions with Dr. S. T. Chui and Dr. T. Ziman and support from the U.S. Department of Energy Office of Basic Energy Sciences, under Contract No. DE-FG02-84ER45082 and the National Sciences and Engineering Research Council (NSERC) of Canada.

*Now at Department of Physics, University of Alberta, Edmonton, Alberta, Canada T6G 2J1.

[1] *Quantum Hall Effect,* edited by R. E. Prange and S. M. Girvin (Springer-Verlag, New York, 1987).

[2] *Two-Dimensional Systems: Physics and New Devices,* Vol. 67 of *Springer Series in Solid-State Sciences,* edited by G. Bauer, F. Kuchar, and H. Heinrich (Springer, Berlin, 1986), p. 204.

[3] T. Ando, A. B. Fowler, and F. Stern, Rev. Mod. Phys. **54**, 437 (1982).

[4] K. von Klitzing, G. Dorda, and M. Pepper, Phys. Rev. Lett. **45**, 494 (1980).

[5] D. C. Tsui, Th. Englert, A. Y. Cho, and A. C. Gossard, Phys. Rev. Lett. **44**, 341 (1980).

[6] Th. Englert, D. C. Tsui, J. C. Portal, J. Beerens, and A. C. Gossard, Solid State Commun. **44**, 1301 (1982).

[7] G. Kido, N. Miura, H. Ohno, and H. Sakaki, J. Phys. Soc. Jpn. **51**, 2168 (1982).

[8] D. Heitmann, M. Ziesmann, and L. L. Chang, Phys. Rev. B **34**, 7463 (1986).

[9] N. Mori, H. Murata, K. Taniguchi, and C. Hamaguchi, Phys. Rev. B **38**, 7622 (1988).

[10] E. Gornik, R. Lassnig, G. Strasser, H. L. Stormer, A. C. Gossard, and W. Wiegmann, Phys. Rev. Lett. **54**, 1820 (1985).

[11] T. P. Smith III, W. I. Wang, and P. J. Stiles, Phys. Rev. B **34**, 2995 (1986).

[12] T. P. Smith III, B. B. Goldberg, P. J. Stiles, and M. Heiblum, Phys. Rev. B **32**, 2696 (1985).

[13] T. Haavasoja, H. L. Stormer, D. J. Bishop, V. Narayanamuriti, A. C. Gossard, and W. Wiegmann, Surf. Sci. **142**, 294 (1984).

[14] E. Stahl, D. Weiss, G. Weimann, K. von Klitzing, and K. Ploog, J. Phys. C **18**, L783 (1985).

[15] J. P. Eisenstein, H. L. Stormer, V. Narayanamurti, A. Y. Cho, A. G. Gossard, and C. W. Tu, Phys. Rev. Lett. **55**, 875 (1985).

[16] M. G. Gavrilov and I. V. Kukushkin, Pis'ma Zh. Eksp. Teor. Fiz. **43**, 79 (1986) [JETP Lett. **43**, 103 (1986)].

[17] J. K. Wang, J. H. Campbell, D. C. Tsui, and A. Y. Cho, Phys. Rev. B **38**, 6174 (1988).

[18] T. Ando, J. Phys. Soc. Jpn. **38**, 989 (1975); T. Ando and Y. Uemura, in *High Magnetic Fields in Semiconductor Physics,* Vol. 71 of *Springer Series in Solid-State Sciences,* edited by G. Landwehr (Springer, Berlin, 1987).

[19] R. R. Gerhardts and V. Gudmundsson, Phys. Rev. B **35**, 8005 (1987); **34**, 2999 (1986).

[20] T. Ando, J. Phys. Soc. Jpn. **43**, 1616 (1977).

[21] S. Das Sarma, Phys. Rev. B **23**, 4592 (1981); S. Das Sarma and X. C. Xie, Phys. Rev. Lett. **61**, 738 (1988).

[22] R. Lassnig and E. Gornik, Solid State Commun. **47**, 959 (1983).

[23] T. Ando and Y. Murayama, J. Phys. Soc. Jpn. **54**, 1519 (1985).

[24] W. Cai and T. S. Ting, Phys. Rev. B **33**, 3967 (1986).

[25] Y. Murayama and T. Ando, Phys. Rev. B **35**, 2252 (1987).

[26] V. Sa-yakanit, N. Choosiri, and H. R. Glyde, Phys. Rev. B **38**, 1340 (1988).

[27] K. Esfarjani, V. Sa-yakanit, and H. R. Glyde, in *Path Integrals from meV to MeV,* edited by W. Sritrakool and V. Sa-yakanit (World Scientific, Singapore, 1989).

[28] I. M. Lifshits, S. A. Gredeskul, and L. A. Pastur, in *Introduction to the Theory of Disordered Systems* (Wiley, New York, 1988).

[29] F. Wegner, Z. Phys. B **51**, 279 (1983); in *High Magnetic Fields in Semiconductor Physics,* Vol. 71 of *Springer Series in Solid State Sciences,* edited by G. Landwehr (Springer, Berlin, 1987).

[30]E. Brézin, D. J. Gross, and C. Itzykson, Nucl. Phys. **B235**, 24 (1984).
[31]I. Affleck, J. Phys. C **17**, 2323 (1984).
[32]A. Klein and J. F. Perez, Nucl. Phys. B **251**, 199 (1985).
[33]W. Apel, J. Phys. C **20**, L577 (1987).
[34]R. R. Gerhardts, Z. Phys. B **21**, 275 (1975); **21**, 285 (1975).
[35]V. Sa-yakanit, Phys. Rev. B **19**, 2266 (1979); T. Lukes, Philos. Mag. **13**, 875 (1966); **12**, 719 (1965); S. F. Edwards and Y. B. Gulyaev, Proc. Phys. Soc. London **83**, 495 (1964); R. P. Feynman and A. R. Hibbs, *Quantum Mechanics and Path Integrals* (McGraw-Hill, New York, 1965).
[36]W. Sritrakool, V. Sa-yakanit, and H. R. Glyde, Phys. Rev. B **33**, 1196 (1986); V. Sa-yakanit and H. R. Glyde, Comments Condensed Matter Phys. **13**, 35 (1987).
[37]K. Broderix, N. Heldt, and H. Leschke, Z. Phys. B **68**, 19 (1987); Phys. Rev. B **40**, 7479 (1989).
[38]S. T. Chui, Phys. Rev. B **34**, 4436 (1986).

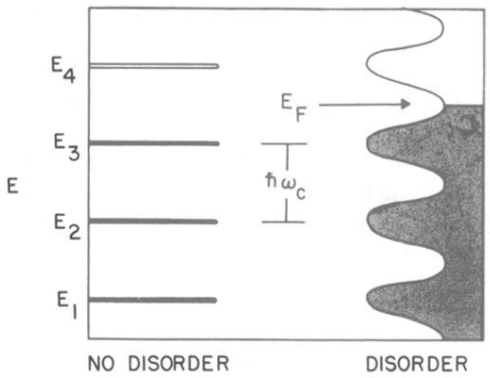

FIG. 2. The Landau levels for no disorder and broadened by disorder according to Eq. (6). The magnetic field B and electron density n_s in the figure is selected so that three LL's are completely filled (filling factor equals 6).